Supplementary Materials

Environmental Justice Assessment of Fine Particles, Ozone, and Mercury over the Pearl River Delta Region, China

Wang Chang [1], Yun Zhu [1,*], Che-Jen Lin [2], Saravanan Arunachalam [3], Shuxiao Wang [4], Jia Xing [4], Tingting Fang [1], Shicheng Long [1], Jinying Li [1] and Geng Chen [5]

[1] Guangdong Provincial Key Laboratory of Atmospheric Environment and Pollution Control, College of Environment and Energy, South China University of Technology, Guangzhou Higher Education Mega Center, Guangzhou 510006, China
[2] Department of Civil and Environmental Engineering, Lamar University, Beaumont, TX 77710, USA
[3] Institute for the Environment, University of North Carolina at Chapel Hill, Chapel Hill, NC 27599, USA
[4] State Key Joint Laboratory of Environmental Simulation and Pollution Control, School of Environment, Tsinghua University, Beijing 100084, China
[5] Guangdong Environmental Monitoring Center, Guangzhou 510308, China
* Correspondence: zhuyun@scut.edu.cn; Tel.: +86-13316253667

1. Air quality in the PRD during China's 13th Five-Year Plan (2016~2020)

Table S1. Air quality in the PRD during the 13th Five-Year Plan period.

Year	AQCI*	$PM_{2.5}$		PM_{10}		NO_2		O_3-8h-90per		SO_2		CO	
		concentration (μg/m³)	contribution (%)	concentration (μg/m³)	contribution (%)	concentration (μg/m³)	contribution (%)	concentration (μg/m³)	contribution (%)	concentration (μg/m³)	contribution (%)	concentration (mg/m³)	contribution (%)
2016	3.6	30	22.35%	45	16.76%	32	20.86%	138	22.49%	10	4.35%	1.1	7.17%
2017	**3.84**	**32**	**23.84%**	**48**	**17.88%**	**34**	**22.16%**	**151**	**24.61%**	**10**	**4.35%**	**1.1**	**7.17%**
2018	3.65	30	22.35%	46	17.13%	32	20.86%	150	24.44%	9	3.91%	1.0	6.52%
2019	3.82	28	20.86%	47	17.51%	33	21.51%	176	28.68%	7	3.04%	1.2	7.82%
2020	3.08	21	15.64%	38	14.15%	26	16.95%	148	24.12%	7	3.04%	0.9	5.87%

Note: Data from Guangdong Environmental Monitoring Center; * AQCI denotes Air Quality Composite Index.

2. Model description

The driving data of the WRF model were 6-hour global meteorological satellite data provided by the National Centers for Environmental Prediction (NCEP), which were assimilated with sounding and ground station observations. The WRF outputs were processed into the ready format for the meteorological fields of the CMAQ model through the Meteorological-Chemical Interface Processor (MCIPv4.3). The configuration parameters of the WRF model in this study are listed in Table S2.

The initial and boundary conditions of the outermost in the CMAQ model were generated based on the default configuration, and the initial and boundary conditions for the middle and inner domains were from the simulation results of the outer and middle domains, respectively. For $PM_{2.5}$ and O_3 concentration simulations, the Carbon Bond version 6 (CB06) was used as the gas-phase chemical mechanism; the criteria air pollutant emission inventories used in the outer and middle domains were provided by Tsinghua University [1,2], and the emission inventory used in the inner domain was developed jointly by Tsinghua University and South China University of Technology. The gas-phase chemical mechanism for the Hg deposition simulation was CB05, and the mercury emission inventory used was updated from the 2014 mercury emission inventory developed in a previous study by our team [3]. The detailed configuration parameters are shown in Table S3.

Table S2. Parameters of main physics processes in WRF v3.9.1.

Physics	Parameterization scheme
Cumulus convection schemes	Kain-Fritsch
Land-Surface schemes	Pleim-Xiu LSM
Planetary boundary layer schemes	ACM2
Longwave radiation schemes	RRTMG
Shortwave radiation schemes	RRTMG
Microphysics schemes	Morrison 2-mom

Table S3. Parameter configurations of CMAQ v5.2.

Parameter	Value
Nested grid	Three nested
Horizontal resolution	27/9/3 km
Vertical layers	14
Horizontal advection	Yamartino global mass-conserving scheme
Horizontal diffusion	Explicit
Vertical advection	Yamartino global mass-conserving scheme
Vertical diffusion	ACM2
Dry deposition	M3DRY
Gas-phase chemistry mechanism	CB06 for $PM_{2.5}$ and O_3 simulation, CB05 for Hg simulation
Gas-phase chemistry algorithm	EBI
Plume in grid	off
Boundary condition	default
Initial condition	default

3. Model results

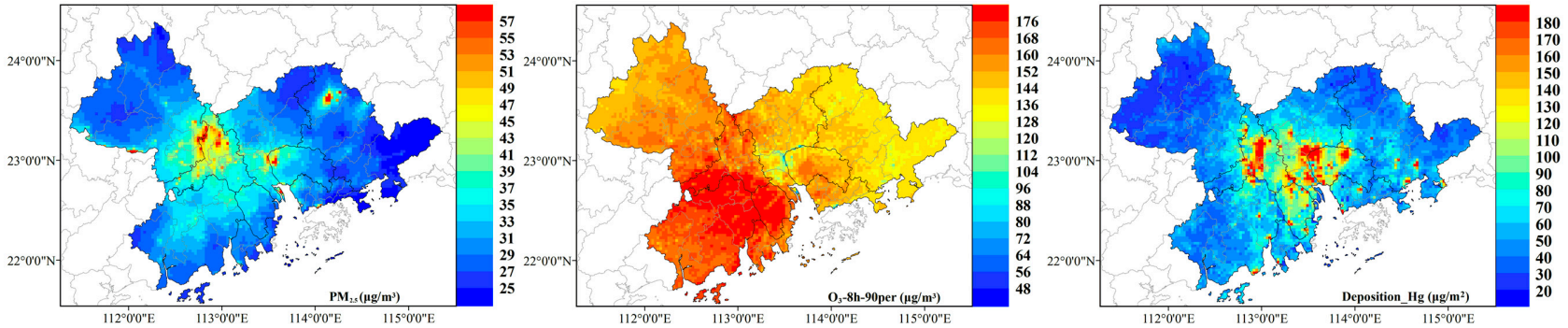

Figure S1. Simulated concentration maps of $PM_{2.5}$ and O_3, and simulated deposition map of Hg. The simulated concentrations of $PM_{2.5}$ and O_3 were assimilated with monitoring data using the DF tool.

4. Model validation

In this study, the observed concentrations from all national air quality monitoring stations in the PRD were compared with the simulated concentrations of $PM_{2.5}$ and O_3 to assess the model performance, and the statistical metrics used are correlation coefficient (R, Equation (S1)) and normalized mean bias (NMB, Equation (S2)) (Table S4). The results of comparing the observed concentrations from the Shundesugang Station, Dayawanguanweihui Station, Mugang Station and Beijie station located in the central, eastern, northern and western PRD, respectively, with the simulated concentrations were randomly selected below to further analyze the model performance (Figure 2b). The validation results show that the simulation and observation results are in good agreement (Figure S2 to Figure S9). The Rs of the simulated versus observed $PM_{2.5}$ (O_3) concentrations in January, April, July and October are 0.638~0.701 (0.62~0.721), 0.658~0.752 (0.715~0.745), 0.605~0.656 (0.767~0.835) and 0.616~0.691 (0.647~0.769) respectively, which are greater than the recommended standard of 0.4 (0.5) [4]; also, the ranges of NMB are −11.84%~22.62% (−13.79%~34.21%), −19.44%~15.97% (−15.43%~6.14%), −8.03%~28.86% (−3.97%~7.71%) and 26.41%~53.57% (−26.5%~4.87%), respectively, which also largely did not exceed the recommended standard value [4].

Since long-term observations of mercury are very scarce in the PRD, we simultaneously compared simulated concentration and deposition of mercury with short-term observation data from the few relevant studies to evaluate the model performance as comprehensively as possible (Table S5). Compared with the concentrations observed by Luo, *et al.* [5] in 2019, the relative bias (Equation (S3)) of the simulated TGM concentration is about −24%, which is at an acceptable level. Nevertheless, compared with the observed concentrations from the studies before 2011, the simulated TGM concentration is smaller, with relative bias ranging from −75.68% to −45.56% [6,7], which is caused by the implementation of a series of industrial pollution control policies in the PRD from 2011 to 2017, such as the "Emission Standards of Non-ferrous Metal Smelting Industry Pollutants" introduced in 2010, "Emission Standards of Iron and Steel Industrial Pollutants" issued in 2012, "Emission Standards of Air Pollutants for Cement Industry" revised in 2013, "Standard for Pollution Control on the Municipal Solid Waste Incineration" revised in 2014, and "Ultra-Low Emission and Energy Saving of Coal-fired Power Plant Plan" implemented in 2015, etc. [8]. As for Hg deposition, the relative biases are −38% and 26.36% compared with the observations of Huang, *et al.* [9] at the Mt. Dinghu site and the Guangzhou site, respectively. This is possibly caused by meteorological factors, for example, the precipitation at the Mt. Dinghu (Guangzhou) site is 1738.4 (1813.9) mm and 1275.5 (1828.8) mm during the observation and simulation year, respectively, which undoubtedly affected the wet deposition of Hg significantly.

$$R = \frac{\sum_{i=1}^{N}(Sim_i - \overline{Sim})\left(Obs_i - \overline{Obs}\right)}{\sqrt{\sum_{i=1}^{N}(Sim_i - \overline{Sim})^2 \sum_{i=1}^{N}\left(Obs_i - \overline{Obs}\right)^2}} \quad \text{(S1)}$$

$$NMB = \frac{\sum_{i=1}^{N}(Sim_i - Obs_i)}{\sum_{i=1}^{N} Obs_i} \quad \text{(S2)}$$

$$Relative\ bias = \frac{Sim - Obs}{Obs} \quad \text{(S3)}$$

where N is the number of samples; Sim_i is the simulated value of sample i; Obs_i is the observed value of sample i; $\overline{Sim}$ is the mean value of all simulated values; $\overline{Obs}$ is the mean value of all observed values; Obs is the observed value; Sim is the simulated value.

Table S4. Comparison of the simulated concentrations in this study with the observed concentrations from the national air quality monitoring stations in the PRD.

Stations	$PM_{2.5}$								O_3							
	R				NMB (%)				R				NMB (%)			
	Jan	Apr	Jul	Oct	Jan	Apr	Jul	Oct	Jan	Apr	Jul	Oct	Jan	Apr	Jul	Oct
Guangya Middle School	0.67	0.61	0.63	0.57	−4.34	11.51	19.26	20.27	0.64	0.57	0.72	0.69	−9.35	14.09	−8.76	8.14
GZ No.5 Middle School	0.69	0.66	0.65	0.51	−3.47	13.74	4.92	3.68	0.60	0.57	0.72	0.73	31.68	14.12	−8.44	8.81
Tianhezhiyou	0.69	0.58	0.62	0.52	6.56	8.29	−11.23	22.22	0.64	0.56	0.73	0.69	19.47	8.67	10.35	2.89
GD Business College	0.62	0.58	0.59	0.55	−7.74	1.52	−14.92	6.63	0.64	0.56	0.76	0.77	19.18	5.20	12.32	9.03
GZ No.86 Middle School	0.68	0.69	0.57	0.57	−2.48	−11.09	−16.94	−18.60	0.64	0.59	0.78	0.73	−15.23	2.18	11.21	10.57
Panyu middle school	0.63	0.66	0.63	0.52	8.97	9.67	−14.00	−11.85	0.53	0.58	0.67	0.78	8.17	−14.70	7.22	2.88
Huadu normal school	0.69	0.73	0.60	0.56	−4.13	4.19	−9.81	−22.16	0.50	0.56	0.70	0.72	−8.41	−6.89	8.76	10.22
GZ monitoring center	0.65	0.71	0.68	0.56	8.08	−3.79	3.07	26.92	0.54	0.58	0.78	0.69	−16.53	−9.70	4.39	6.94
Jiulong town	0.64	0.63	0.68	0.53	−7.21	−7.74	−3.74	−24.15	0.54	0.61	0.76	0.75	−14.89	7.56	5.18	−1.78
Luhu	0.68	0.69	0.63	0.60	−2.45	−3.04	−7.20	17.28	0.54	0.58	0.76	0.73	−24.09	17.86	−4.00	2.57
Maofeng mountain	0.69	0.65	0.57	0.56	−9.64	3.06	−14.29	−4.55	0.60	0.64	0.68	0.72	−9.05	−15.01	−7.91	−20.01
Tiyuxi	0.68	0.70	0.56	0.54	9.91	−13.20	−8.89	6.72	0.55	0.63	0.68	0.70	27.99	17.92	1.58	−15.52

Liyuan	0.62	0.72	0.64	0.55	14.22	−2.64	14.40	10.69	0.52	0.57	0.71	0.68	−5.69	11.90	−5.54	5.83
Honghu	0.64	0.65	0.59	0.53	−2.73	16.30	10.70	10.04	0.53	0.60	0.69	0.74	21.78	11.26	−2.24	7.00
Huaqiaocheng	0.66	0.71	0.65	0.58	−3.03	−10.83	8.22	7.29	0.55	0.56	0.75	0.75	14.38	−1.07	−6.26	−7.42
Nanyou	0.64	0.67	0.61	0.53	14.08	3.38	−17.76	1.11	0.56	0.56	0.76	0.70	20.99	18.78	−15.41	17.29
Yantian	0.62	0.69	0.67	0.53	7.44	9.88	−8.34	−2.00	0.61	0.56	0.76	0.79	19.75	−17.30	−9.22	−4.21
Longgang	0.61	0.67	0.63	0.54	−3.79	3.35	8.03	34.91	0.63	0.63	0.68	0.71	−15.93	−14.83	7.59	2.85
Xixiang	0.69	0.60	0.57	0.51	10.29	−4.82	3.66	7.58	0.51	0.59	0.69	0.78	29.14	−14.76	−8.57	−9.38
Nanao	0.64	0.57	0.57	0.55	−5.29	11.53	−3.87	3.15	0.64	0.65	0.72	0.70	18.58	−17.95	2.26	−2.32
Kuichong	0.60	0.60	0.61	0.55	7.76	8.05	−10.42	−7.23	0.57	0.58	0.74	0.74	25.43	−2.39	−5.54	−3.81
Meisha	0.66	0.60	0.64	0.51	−4.87	15.82	−16.34	−15.14	0.50	0.59	0.69	0.73	15.07	−8.85	−8.85	−6.42
Guanlan	0.67	0.71	0.60	0.53	9.06	−11.27	9.00	−24.39	0.58	0.63	0.70	0.78	−16.15	−11.23	11.93	3.87
Huaboyuan	0.68	0.64	0.57	0.57	11.99	5.79	15.79	−15.96	0.64	0.57	0.77	0.69	28.08	−16.07	−13.48	−9.68
Zhangxi	0.67	0.67	0.60	0.55	10.41	8.22	9.51	−11.04	0.63	0.65	0.76	0.76	−5.55	−6.03	−10.23	−8.06
Zimaling	0.69	0.60	0.57	0.52	−2.13	3.75	−7.68	−14.74	0.62	0.59	0.71	0.68	12.01	12.47	−7.54	−11.04
YangtzeTourism	0.69	0.55	0.67	0.54	9.91	−13.12	15.24	20.10	0.62	0.62	0.75	0.80	−16.49	−16.68	12.75	5.11
Dongchengzhushan	0.67	0.67	0.56	0.52	−7.32	9.92	13.23	−16.99	0.65	0.58	0.76	0.70	14.72	7.95	−1.24	−9.14

Nanchengyuanling	0.61	0.56	0.55	0.54	10.98	17.36	10.05	17.33	0.61	0.55	0.68	0.77	−17.24	−5.55	14.50	9.96
Guanchenglichuan	0.70	0.57	0.68	0.54	6.70	7.79	−9.04	−17.43	0.63	0.60	0.70	0.72	12.00	7.36	−10.62	10.33
Dongchengshijing	0.63	0.65	0.69	0.54	9.16	9.92	11.09	−20.77	0.51	0.61	0.70	0.69	28.61	8.63	−5.27	−3.03
Nanchengxiping	0.63	0.57	0.65	0.51	−5.37	9.27	12.45	−4.36	0.57	0.61	0.67	0.74	−9.78	−12.17	10.66	−6.29
Wanliang	0.67	0.70	0.68	0.53	−6.90	5.55	2.18	16.33	0.63	0.56	0.72	0.79	−12.17	−12.83	3.97	4.53
Huacaizhizhong	0.65	0.72	0.69	0.53	4.23	−8.14	11.97	19.42	0.58	0.60	0.70	0.75	24.02	5.11	−14.55	−6.03
Nanhaiqixiangju	0.69	0.73	0.55	0.51	17.96	23.46	32.78	41.13	0.57	0.63	0.73	0.76	−12.38	−14.30	−13.86	2.06
Shundesugang	**0.64**	**0.67**	**0.61**	**0.62**	**1.99**	**15.97**	**24.27**	**53.57**	**0.72**	**0.74**	**0.80**	**0.77**	**−13.79**	**−15.43**	**0.26**	**−26.50**
Ronggui	0.64	0.55	0.62	0.57	7.40	−7.51	−13.88	−22.78	0.64	0.58	0.70	0.72	−7.85	−15.37	1.03	3.00
Gaomingkongtang	0.64	0.68	0.58	0.54	−6.45	−5.49	−3.20	−12.45	0.60	0.56	0.72	0.69	−12.87	−13.77	4.58	−3.91
Sanshui monitoring center	0.61	0.65	0.69	0.57	2.55	−13.58	14.77	−13.44	0.62	0.60	0.72	0.75	17.95	16.43	13.24	−1.71
Sanshuiyundonghai	0.69	0.67	0.62	0.56	4.52	3.81	−6.04	20.58	0.58	0.56	0.75	0.67	24.97	−11.65	−9.10	7.32
Mugang	**0.70**	**0.75**	**0.66**	**0.69**	**3.03**	**−14.37**	**−8.03**	**47.36**	**0.71**	**0.72**	**0.79**	**0.74**	**34.21**	**6.14**	**7.05**	**4.87**
Chengzhongzi	0.62	0.64	0.58	0.51	−5.68	1.80	15.25	33.30	0.51	0.59	0.70	0.71	22.79	12.50	−5.65	21.87
Kengkouzi	0.70	0.55	0.70	0.54	−14.23	−22.56	23.02	57.32	0.63	0.57	0.69	0.76	23.73	12.08	−13.96	7.95
Qixingyan	0.60	0.65	0.67	0.58	10.22	−4.44	−12.63	−20.03	0.62	0.60	0.71	0.67	35.85	17.96	−2.05	3.34

Jida	0.67	0.56	0.60	0.58	5.76	1.66	−3.66	10.72	0.52	0.60	0.75	0.76	−17.42	−11.35	9.91	12.00
Qianshan	0.61	0.70	0.67	0.53	−1.70	−1.35	7.09	−10.37	0.52	0.63	0.67	0.66	24.78	−19.76	6.83	10.84
Tangjia	0.69	0.62	0.56	0.59	−15.37	−12.72	−2.22	23.92	0.62	0.58	0.68	0.75	−20.74	16.41	6.30	9.25
Doumen	0.63	0.66	0.64	0.58	11.45	5.01	−18.66	−16.68	0.63	0.55	0.67	0.72	6.99	12.00	6.81	8.35
Beijie	**0.66**	**0.66**	**0.60**	**0.64**	**22.62**	**−0.32**	**18.22**	**47.60**	**0.62**	**0.72**	**0.84**	**0.65**	**16.86**	**−10.56**	**−3.97**	**−13.60**
Xiqu	0.69	0.67	0.61	0.52	−9.03	6.30	13.78	28.52	0.59	0.60	0.70	0.73	14.55	6.10	9.55	−7.28
Guifengxi	0.68	0.66	0.66	0.52	14.64	3.31	−14.87	−23.20	0.52	0.59	0.72	0.75	26.13	2.52	3.06	5.82
Donghu	0.65	0.64	0.58	0.57	−9.75	11.30	23.91	−43.83	0.51	0.60	0.71	0.74	27.21	16.25	−12.52	7.42
Jingshanhu	0.63	0.70	0.65	0.52	7.40	1.79	−14.95	30.36	0.54	0.65	0.68	0.67	−12.45	−7.39	5.51	2.95
Hengjiangsanlu	0.61	0.70	0.65	0.56	−23.45	−10.62	−13.19	−7.92	0.59	0.56	0.77	0.75	26.92	3.26	−8.97	2.30
Jianbeiyunshanxilu	0.64	0.69	0.55	0.54	−8.80	−11.24	14.61	14.85	0.53	0.56	0.67	0.69	17.72	−14.78	−11.74	−6.28
Chuanhu	0.61	0.64	0.70	0.56	12.87	16.70	19.89	25.89	0.59	0.60	0.67	0.77	24.38	11.09	11.70	11.83
Dayawanguanweihui	**0.70**	**0.69**	**0.65**	**0.66**	**−11.84**	**−19.44**	**28.86**	**26.41**	**0.71**	**0.72**	**0.77**	**0.77**	**10.95**	**−3.69**	**7.71**	**−4.76**

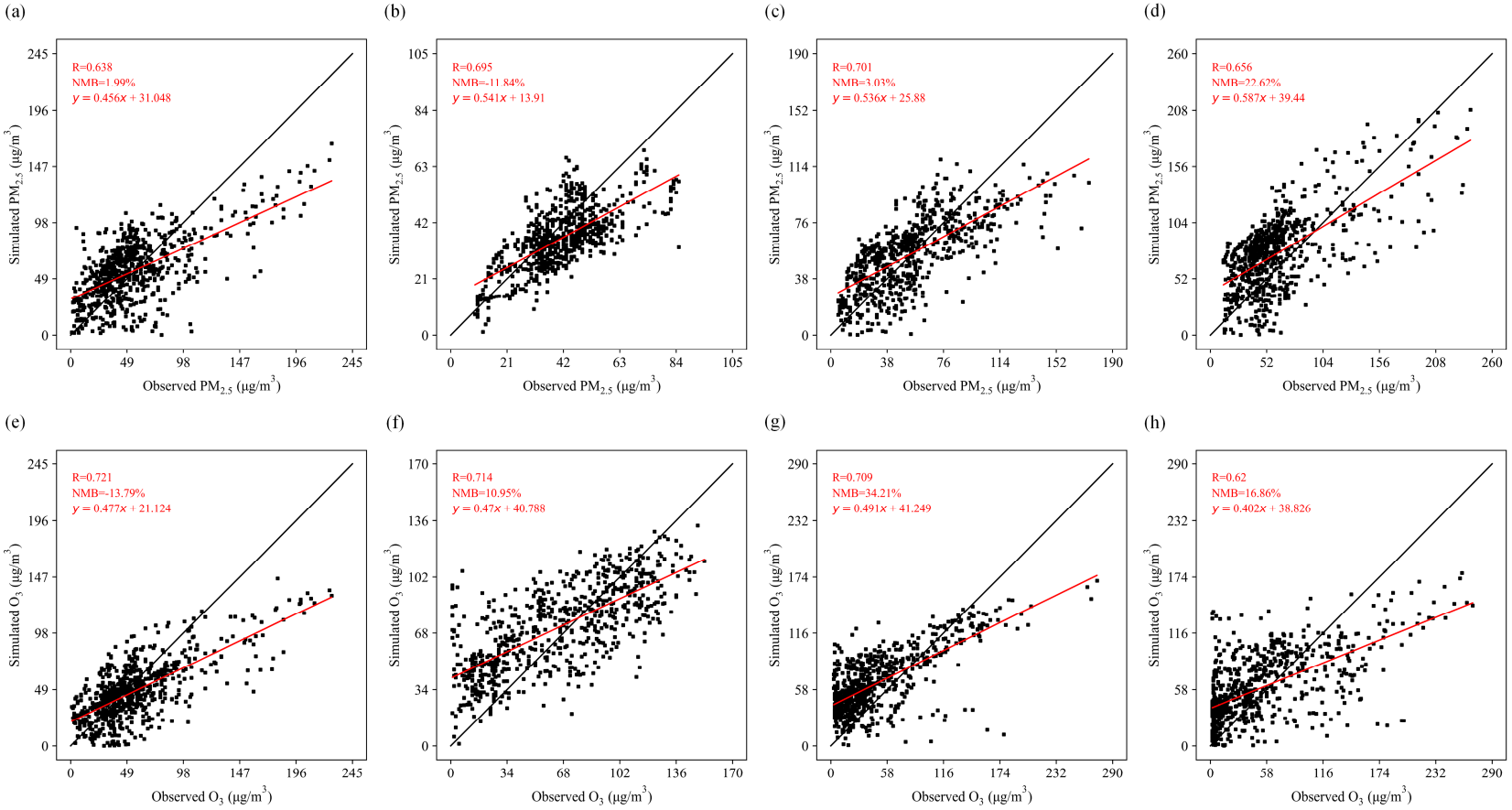

Figure S2. Scatter plots of simulated and observed $PM_{2.5}$ and O_3 concentrations at Shundesugang Station in FS (a, e), Dayawanguanweihui Station in HZ (b, f), Mugang Station in ZQ (c, g), and Beijie Station in JM (d, h) in January.

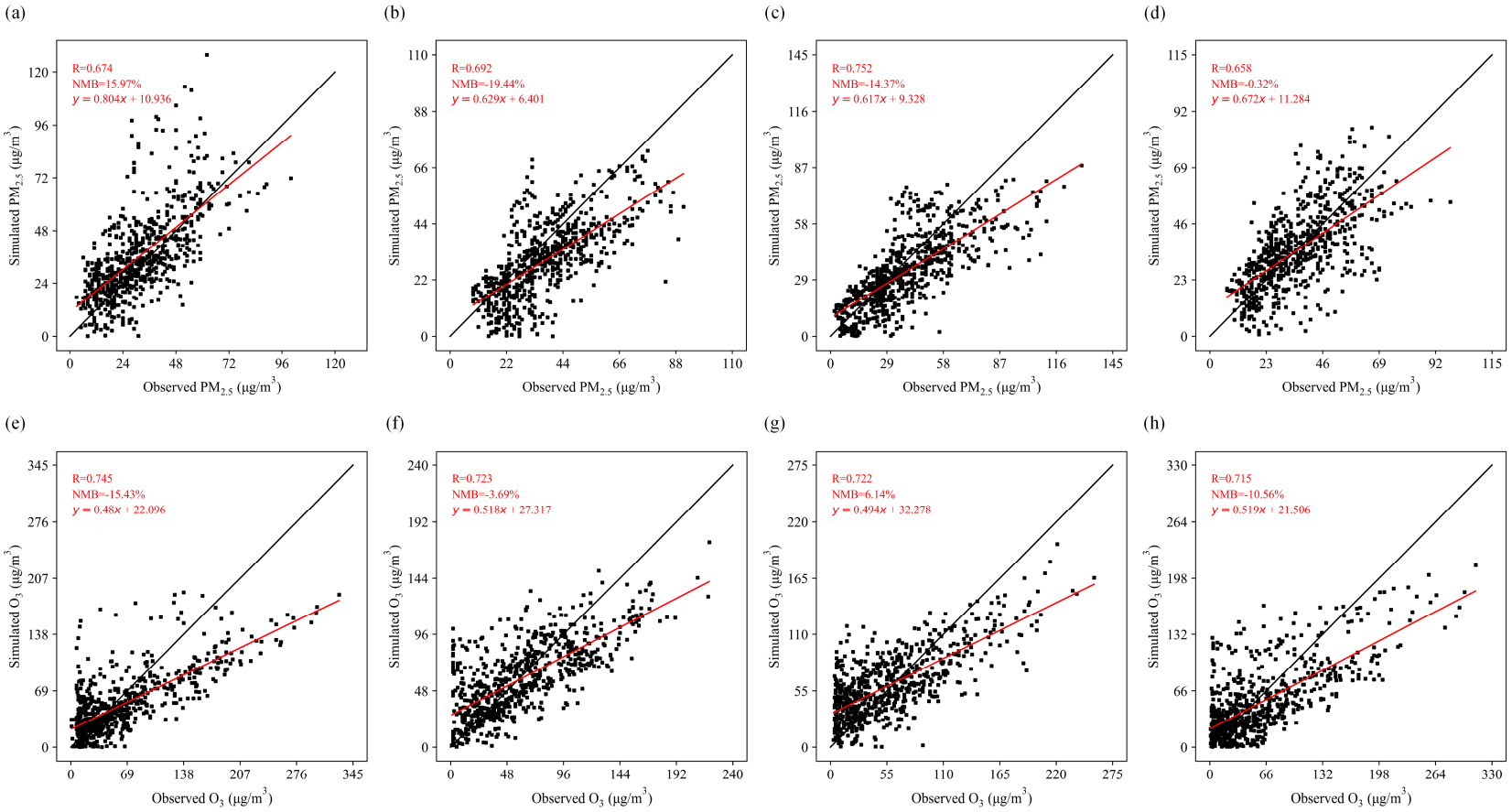

Figure S3. Scatter plots of simulated and observed $PM_{2.5}$ and O_3 concentrations at Shundesugang Station in FS (a, e), Dayawanguanweihui Station in HZ (b, f), Mugang Station in ZQ (c, g), and Beijie Station in JM (d, h) in April.

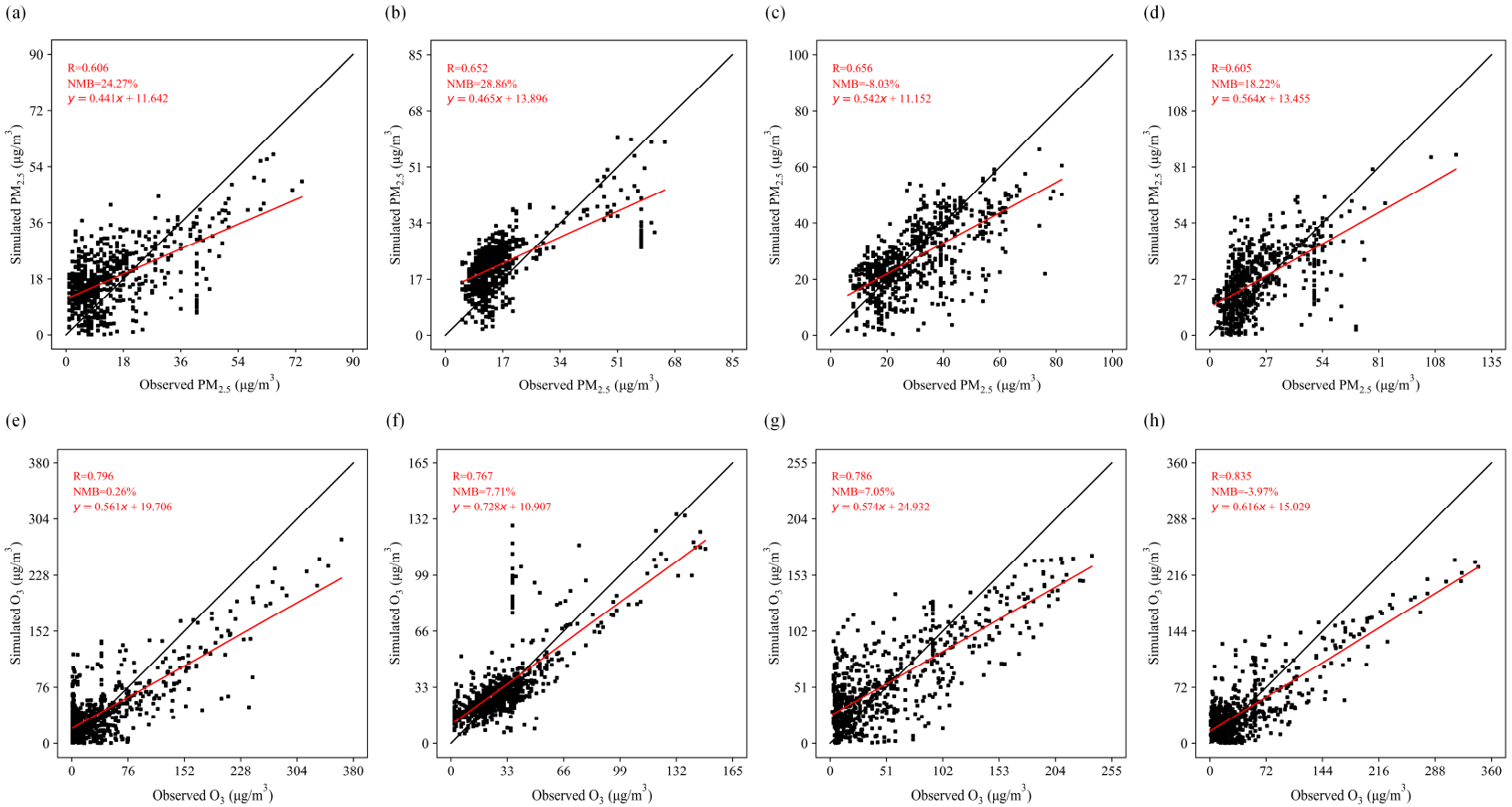

Figure S4. Scatter plots of simulated and observed $PM_{2.5}$ and O_3 concentrations at Shundesugang Station in FS (a, e), Dayawanguanweihui Station in HZ (b, f), Mugang Station in ZQ (c, g), and Beijie Station in JM (d, h) in July.

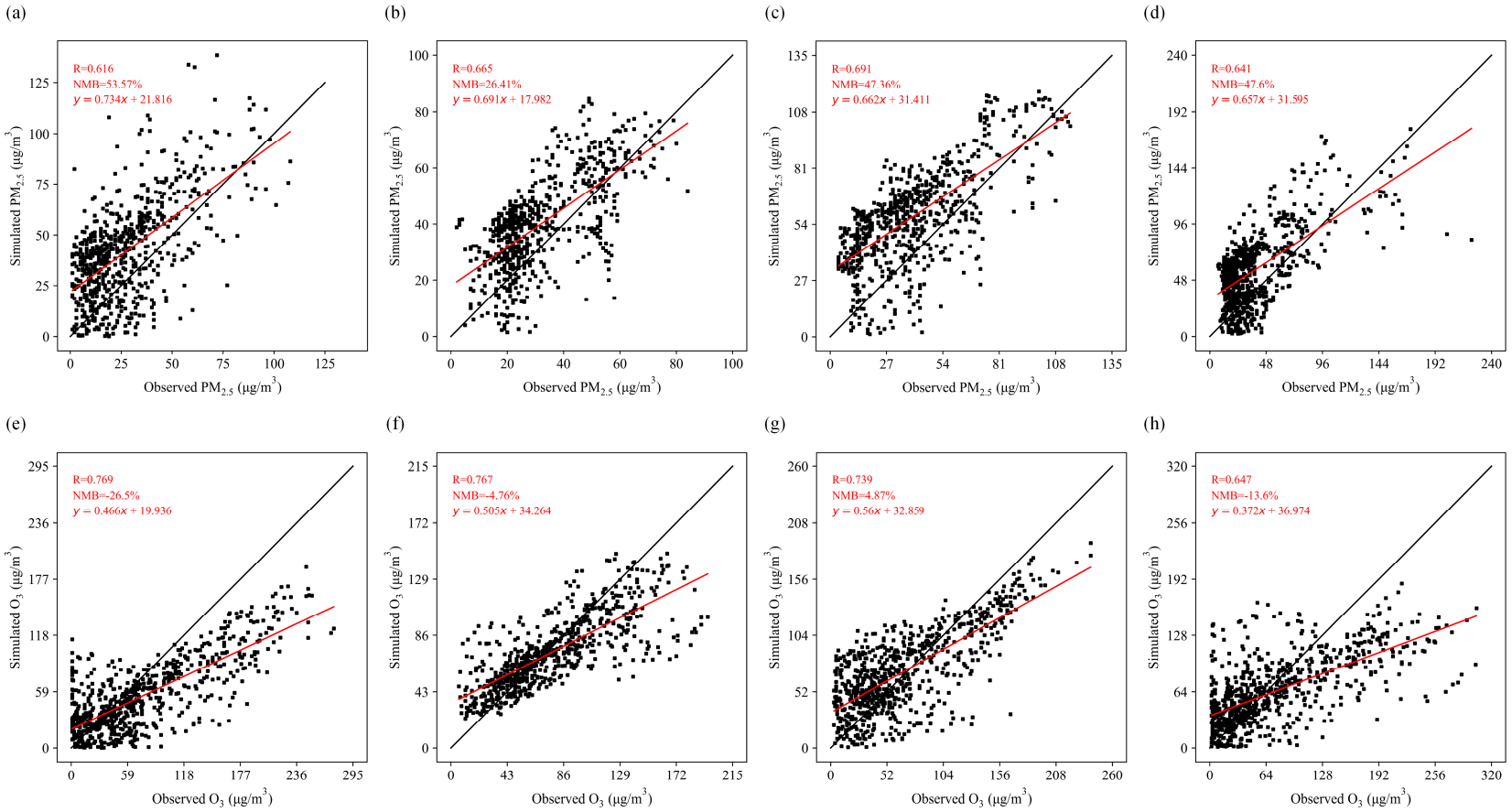

Figure S5. Scatter plots of simulated and observed $PM_{2.5}$ and O_3 concentrations at Shundesugang Station in FS (a, e), Dayawanguanweihui Station in HZ (b, f), Mugang Station in ZQ (c, g), and Beijie Station in JM (d, h) in October.

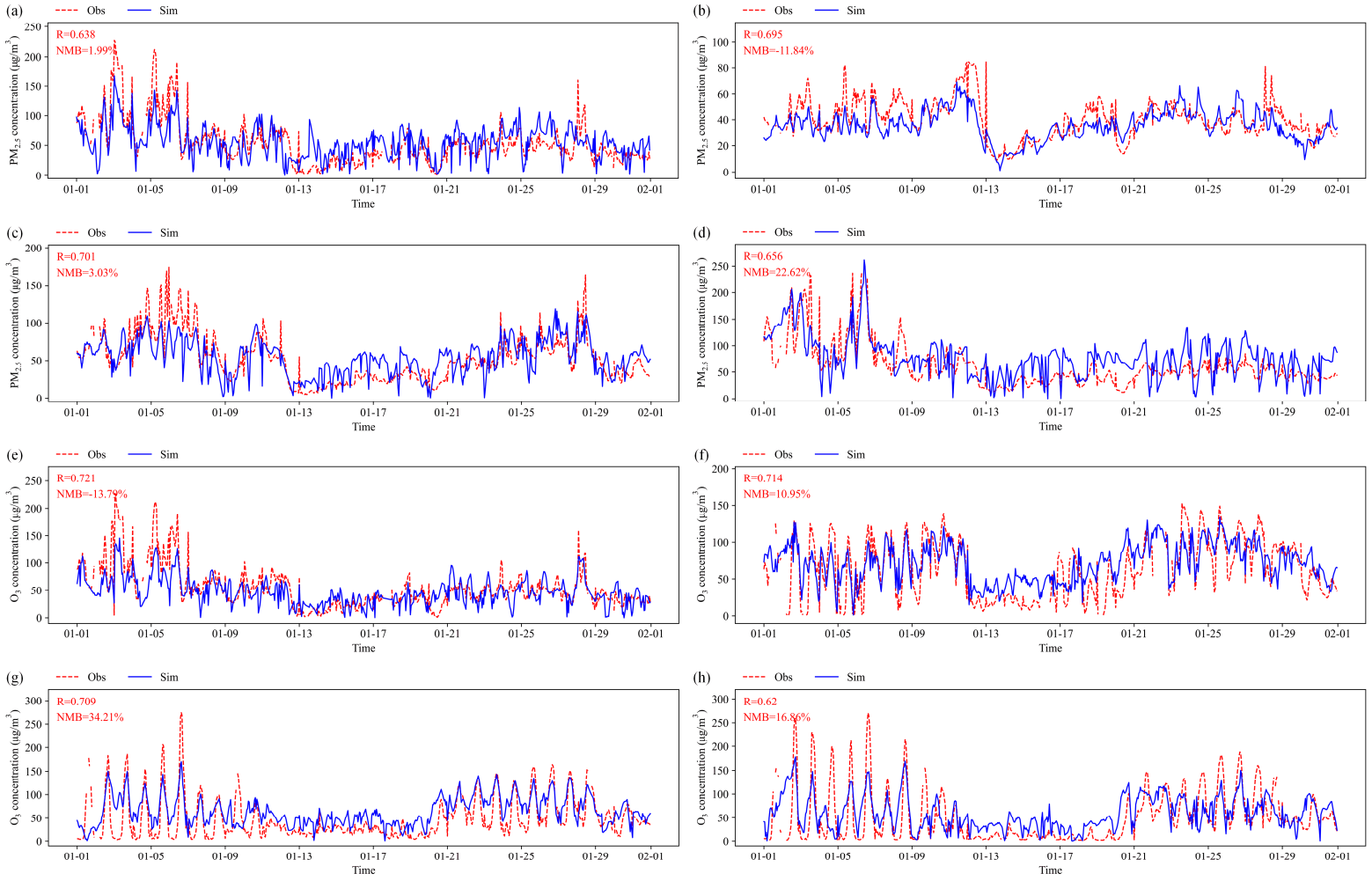

Figure S6. Time series plots of simulated and observed $PM_{2.5}$ and O_3 concentrations at Shundesugang Station in FS (a,e), Dayawanguanweihui Station in HZ (b, f), Mugang Station in ZQ (c, g), and Beijie Station in JM (d, h) in January.

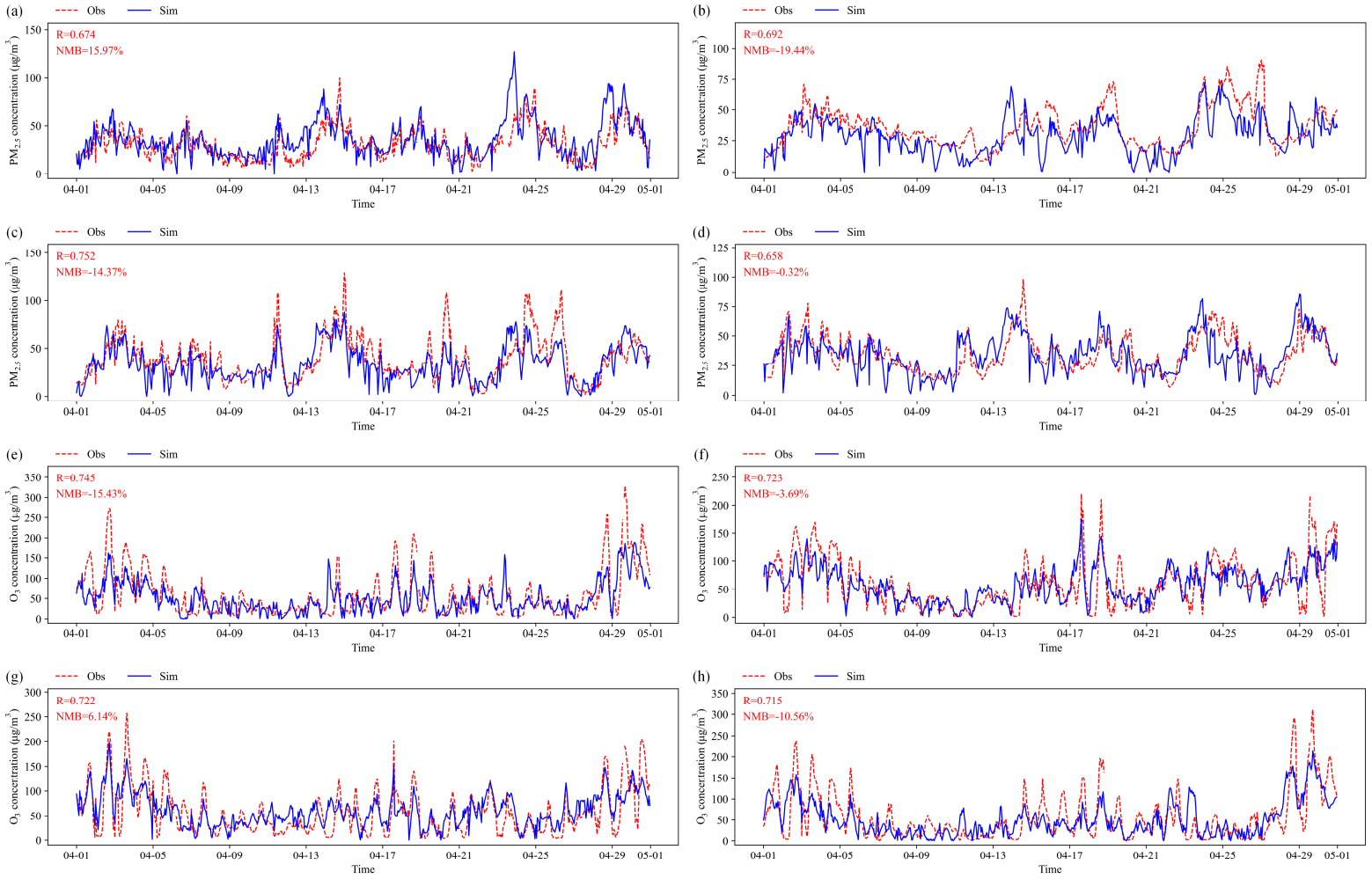

Figure S7. Time series plots of simulated and observed $PM_{2.5}$ and O_3 concentrations at Shundesugang Station in FS (a,e), Dayawanguanweihui Station in HZ (b, f), Mugang Station in ZQ (c, g), and Beijie Station in JM (d, h) in April.

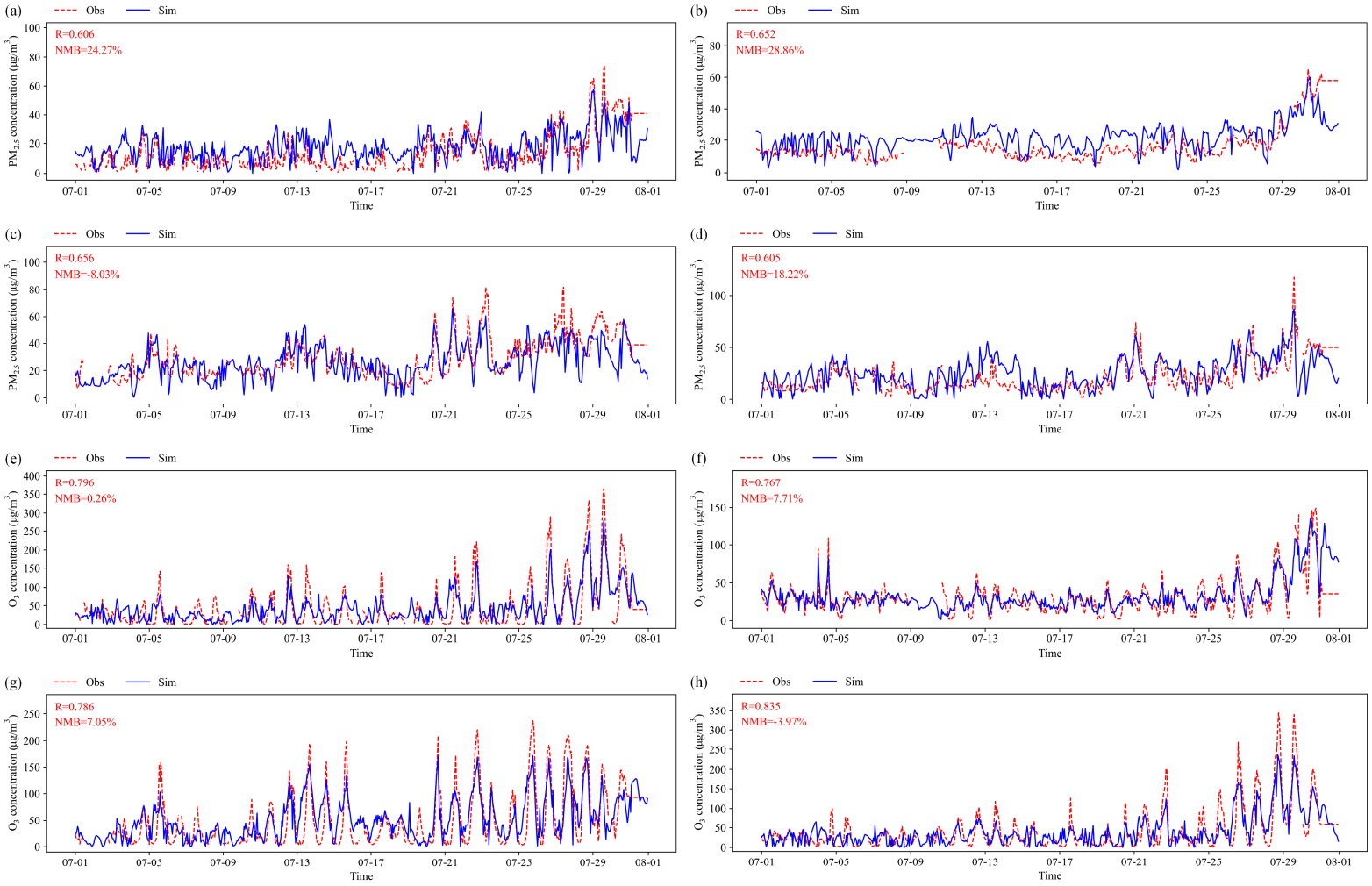

Figure S8. Time series plots of simulated and observed $PM_{2.5}$ and O_3 concentrations at Shundesugang Station in FS (a,e), Dayawanguanweihui Station in HZ (b, f), Mugang Station in ZQ (c, g), and Beijie Station in JM (d, h) in July.

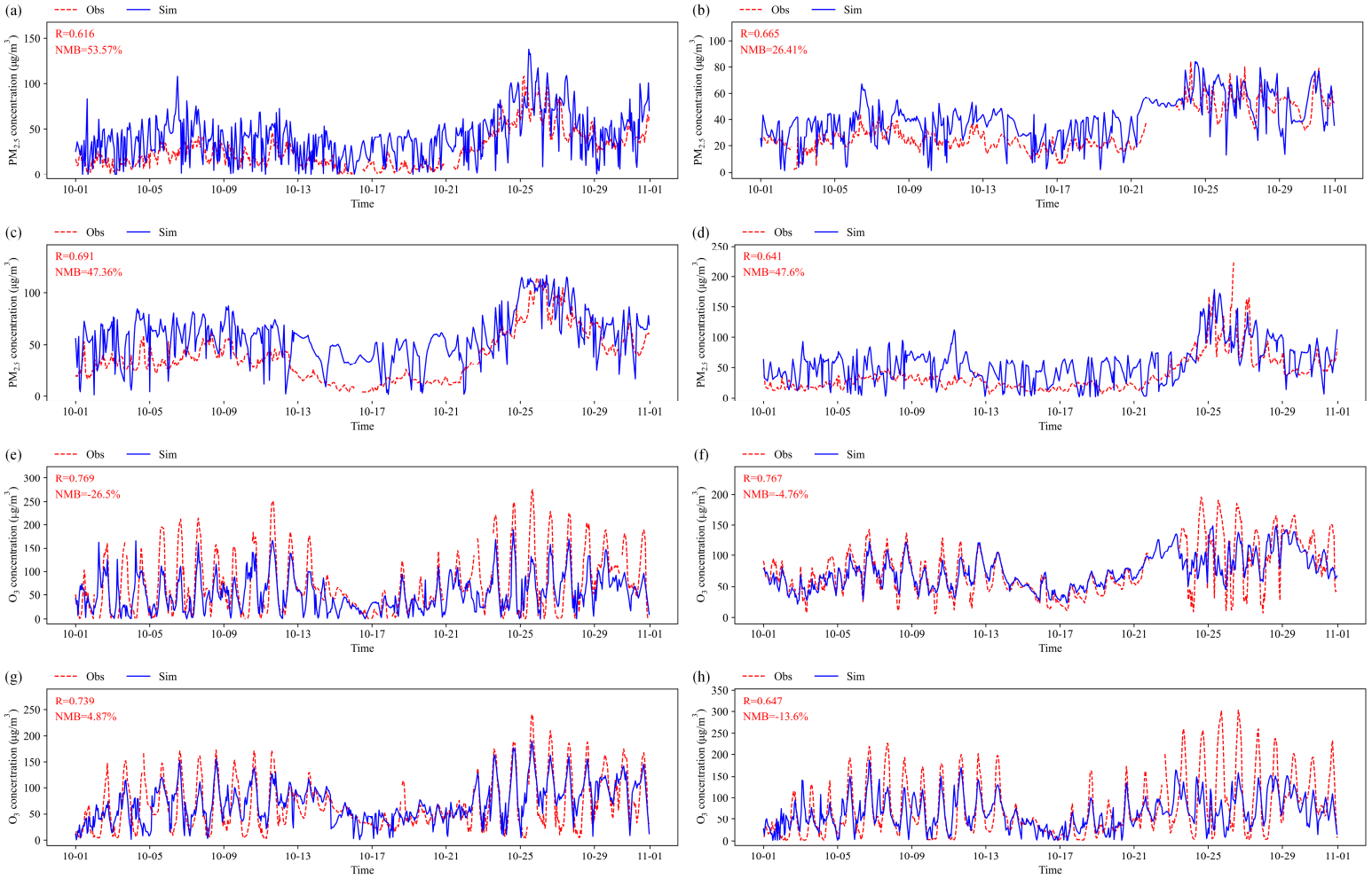

Figure S9. Time series plots of simulated and observed $PM_{2.5}$ and O_3 concentrations at Shundesugang Station in FS (a,e), Dayawanguanweihui Station in HZ (b, f), Mugang Station in ZQ (c, g), and Beijie Station in JM (d, h) in October.

Table S5. Comparison of the simulated Hg concentration and deposition with field measurements in the PRD.

Sites	Longitude	Latitude	Monitoring period	Observation		Simulation		Relative bias
				TGM/GEM (ng/m^3)	Deposition ($\mu g/m^2 \cdot a^{-1}$)	TGM/GEM (ng/m^3)	Deposition* ($\mu g/m^2 \cdot a^{-1}$)	
s41 [5]	113.255	22.649	29/07/2019-30/07/2019	2.10	-	1.59	-	−24.40%
s77 [5]	113.182	22.592	29/07/2019-30/07/2019	2.10	-	1.58	-	−24.69%
Guangzhou obs site [6]	113.355	23.124	11/2010-10/2011	4.60±1.36	-	2.50	-	−45.56%
Mt. Dinghu [6]	112.549	23.164	10/2009-04/2010	5.07±2.89	-	2.39	-	−52.86%
Guangzhou, China [7]	113.050	23.033	01/2005	13.5±7.10	-	3.28	-	−75.68%
Mt. Dinghu [9]	112.549	23.164	2010	-	294.30	-	182.48	−38.00%
Guangzhou, China [9]	113.050	23.033	2012	-	321.19	-	405.84	26.36%

Note: * Hg deposition during the simulation period (i.e., January, April, July and October) was converted into annual Hg deposition when evaluating model performance.

5. Inequality curve

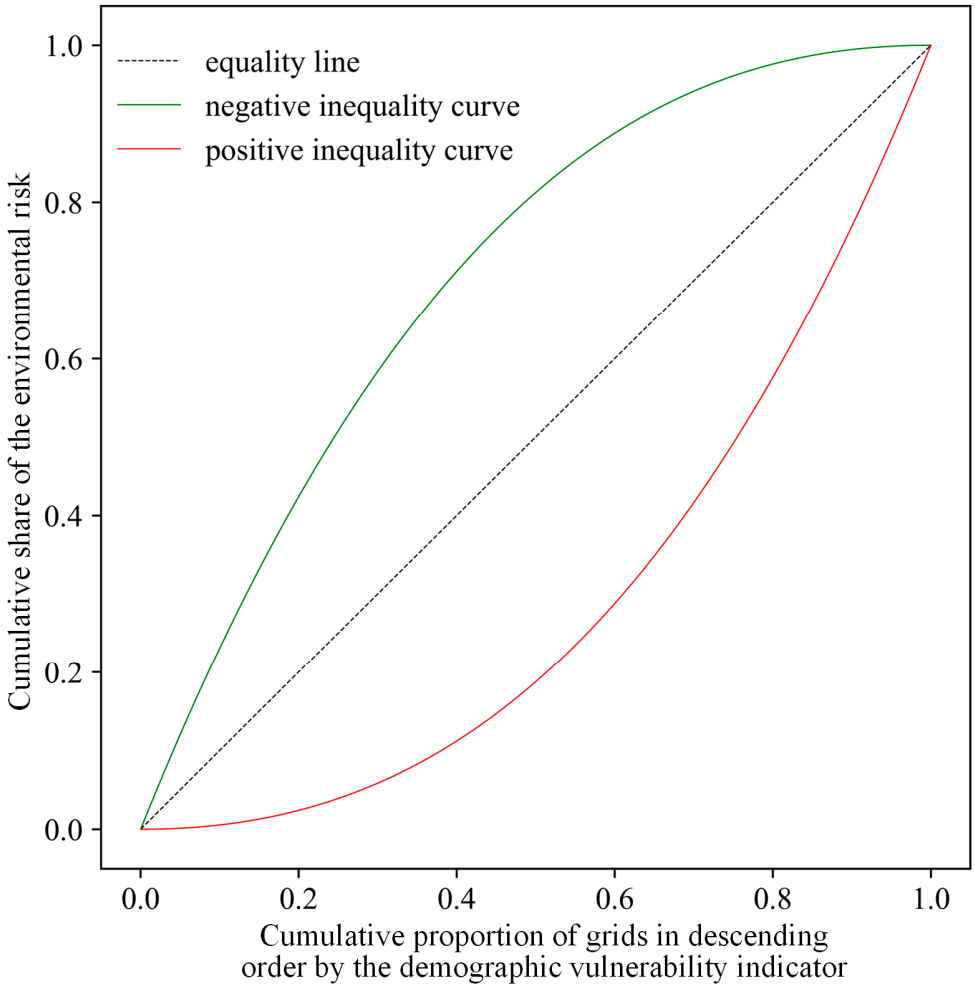

Figure S10. Hypothetical graph of the inequality curve.

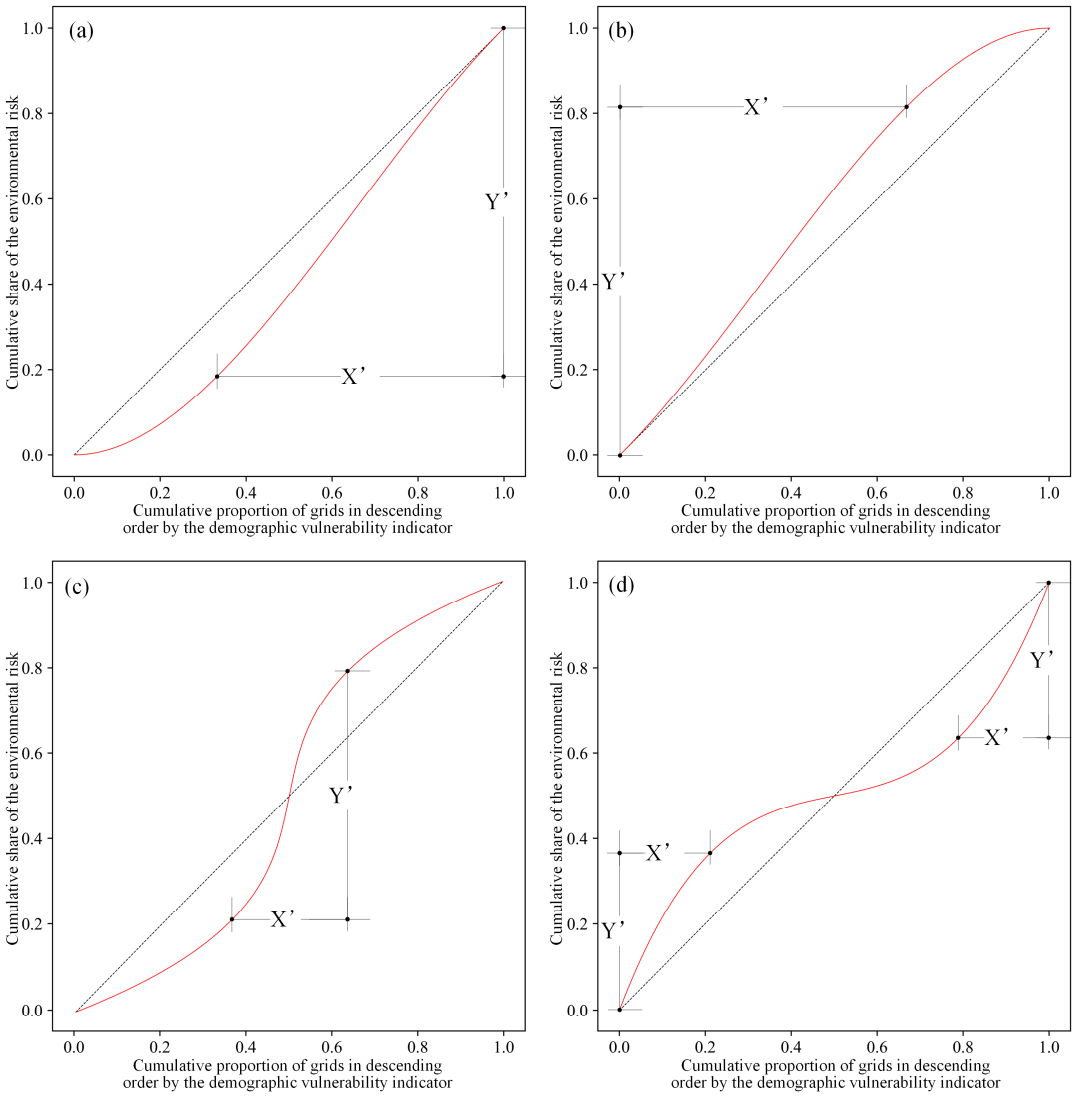

Note: X′ represents overburdened grids, Y′ represents the environmental risk burdened by X′.

Figure S11. Example graphs for identification of environmental risk overburdened areas.

6. Selection of demographic vulnerability indicators

Vulnerable groups who tend to be more vulnerable to environmental pollution are divided into physically vulnerable and socially vulnerable groups. The results of China's 1% Population Sample Survey in 2015 indicate that 16.15% and 10.47% of the total population were over 60 and 65 years old respectively [10], and it is more likely that the percentage of the aging population will increase to approximately 30% in 2050 [11]. Therefore, the Chinese government has issued the two-child policy and the three-child policy one after another [12], and some baby booms are expected to come [13]. On another hand, the elderly are more vulnerable to environmental pollution, usually because their organ functions, metabolic capacity and immunity are declining [14-16]. Children have a poor capacity to physiologically adapt to environmental stress and are susceptible to the adverse effects of air pollution, mainly because of their immature organ systems, lower body weight and higher breathing rates [17-19]. Considering the current status of China's population, and the susceptibility of the elderly & children [20-22], the percentage of the population aged under 14 years & over 65 years was selected as a demographic vulnerability indicator representing the physically vulnerable groups in this study. On the other hand, since the increasing gap between the rich and poor is one of the most serious social problems in China [23], and the poor have a relatively poor ability to avoid environmental risks [24,25], the percentage of the population with low income was chosen as a demographic vulnerability indicator representing socially vulnerable groups. In this study, the group receiving minimum living security funds is regarded as the low-income group. The data sources for the demographic vulnerability indicators mentioned above include the 2010 census results, 2017 statistical yearbooks and 2017 government work reports from each district in the PRD.

7. Information on the socioeconomic and population of the PRD cities

Table S6. The information on education, residents' income, unemployment, and the economy in the PRD cities.

City	Illiterate (%)	Primary school degree (%)	Middle school degree (%)	High school degree (%)	College degree or above (%)	Per capita disposable income (CNY)	Unemployment (%)	GDP per capita (CNY)
GZ	0.95%	15.72%	36.13%	22.92%	19.23%	50782.2	2.40%	150678
FS	1.36%	20.66%	43.61%	19.38%	9.47%	45813.3	2.35%	124324
ZS	1.29%	19.65%	44.98%	21.00%	7.78%	43553.7	2.30%	106327
DG	0.64%	13.50%	54.40%	20.30%	7.10%	45450.6	2.24%	91329
SZ	0.48%	8.88%	44.05%	23.97%	17.18%	52938.0	2.20%	183127
ZH	1.40%	16.18%	33.30%	24.58%	18.39%	44043.1	2.28%	134500
ZQ	2.31%	29.04%	43.54%	11.88%	4.33%	22360.0	2.38%	53674
JM	1.82%	24.33%	42.78%	19.73%	5.36%	26850.6	2.38%	59089
HZ	1.88%	21.93%	48.31%	15.37%	5.75%	31090.6	2.36%	80205

Note: The data on residents' education is from the 2010 census results, and the other data are from the 2017 statistical bulletin of each local government in the PRD.

8. Distributions of major mercury sources

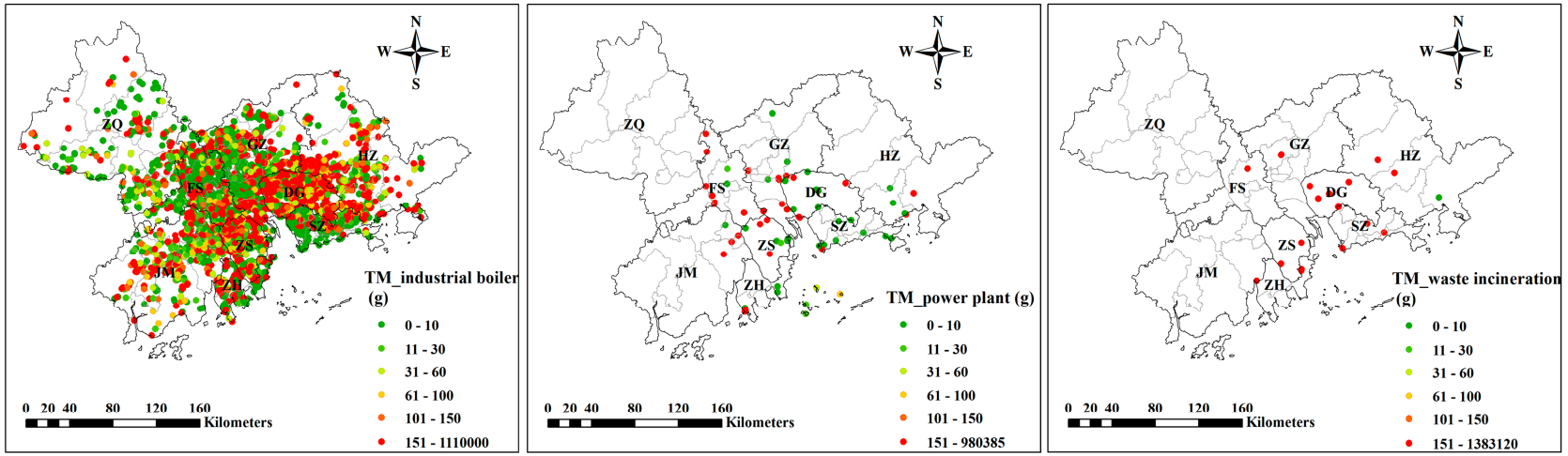

Note: TM denotes total mercury.

Figure S12. Distribution maps of major mercury sources.

9. EI and EI-Hg

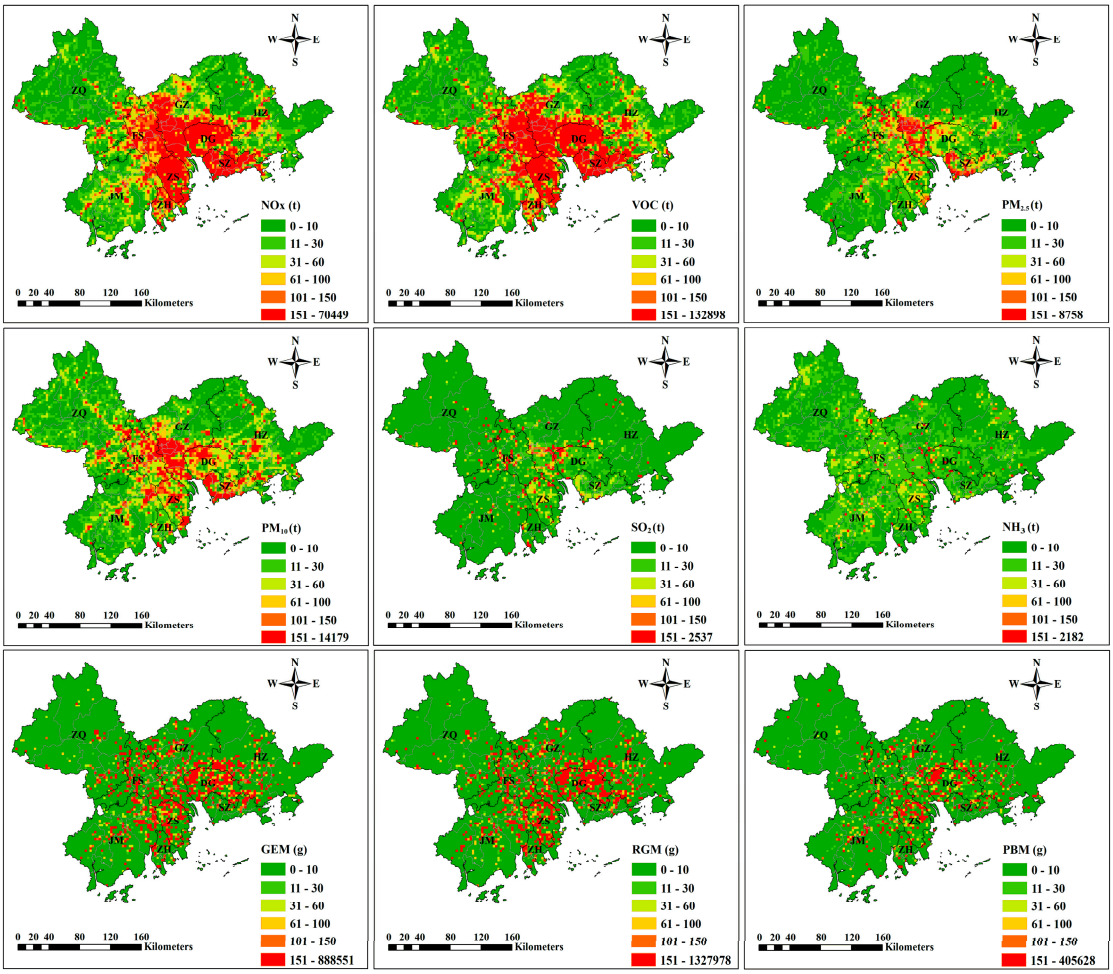

Note: GEM denotes gaseous element mercury, RGM denotes reactive gaseous mercury, and PBM denotes particle-bound mercury.

Figure S13. The EI of criteria air pollutants and the EI of Hg in the PRD region in 2017.

10. Environmental risk indicators

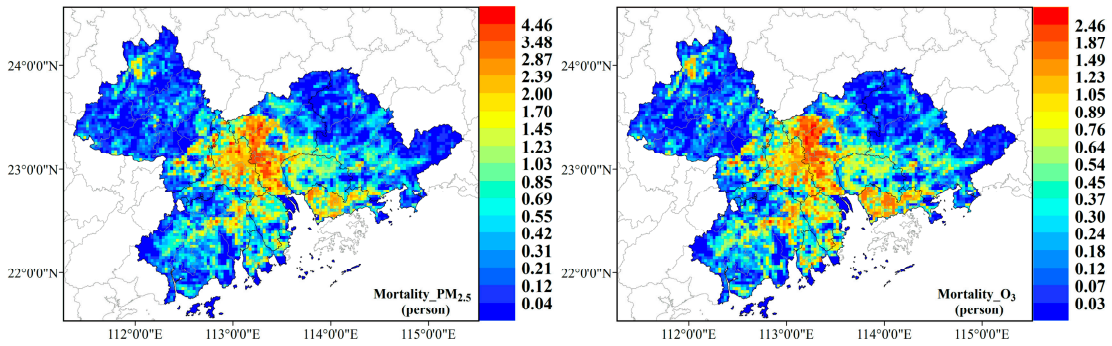

Figure S14. The spatial distributions of environmental risk indicators (Hg deposition is shown in Figure S1).

11. CERS

Table S7. The district-level CERSs in the PRD region.

City	District	CERS based on the % of low income	CERS based on the % of elderly & children
JM	PJ	0.0170	0.0778
JM	JH	0.0229	0.0372
JM	XH	0.1488	0.2477
JM	TS	0.1985	0.2397
JM	KP	0.1160	0.1861
JM	HS	0.0833	0.1015
JM	EP	0.1058	0.1213
HZ	HC	0.0576	0.1380
HZ	HY	0.0591	0.1128
HZ	HuD	0.1837	0.1935
HZ	BL	0.1129	0.2030
HZ	LM	0.1307	0.0945
ZQ	DZ	0.0050	0.0419
ZQ	DH	0.0320	0.0902
ZQ	SH	0.1169	0.1374
ZQ	GY	0.0657	0.2346
ZQ	GN	0.0490	0.1735
ZQ	DQ	0.0282	0.1216
ZQ	FK	0.0482	0.1701
ZQ	HJ	0.1139	0.4062
FS	CC	0.0077	0.0717
FS	NH	0.1092	0.2598
FS	SD	0.0654	0.1616
FS	GaM	0.0715	0.1058
FS	SaS	0.0578	0.1624
GZ	LW	0.0270	0.0730
GZ	ZC	0.0828	0.1611
GZ	CH	0.0890	0.1199
GZ	YX	0.0128	0.0522
GZ	HaZ	0.0236	0.0670
GZ	TH	0.0026	0.0561
GZ	BY	0.0589	0.1697
GZ	HP	0.0249	0.1118
GZ	PY	0.0654	0.1780
GZ	HD	0.0306	0.2369
GZ	NS	0.0604	0.1446
DG	DG	0.1256	0.0893
ZS	ZS	0.0999	0.2133
ZH	XZ	0.0170	0.0434
ZH	DM	0.0308	0.0765
ZH	JW	0.0314	0.0346
SZ	FT	0.0000	0.0145

SZ	LH	0.0009	0.0076
SZ	YT	0.0039	0.0056
SZ	NaS	0.0003	0.0431
SZ	BA	0.0034	0.0095
SZ	LG	0.0038	0.0607
SZ	GM	0.0816	0.0056
SZ	PS	0.0043	0.0075
SZ	LoH	0.0008	0.0000

Reference

1. Zhao, B.; Zheng, H.; Wang, S.; Smith, K.R.; Lu, X.; Aunan, K.; Gu, Y.; Wang, Y.; Ding, D.; Xing, J.; et al. Change in household fuels dominates the decrease in PM2.5 exposure and premature mortality in China in 2005–2015. *Proceedings of the National Academy of Sciences - PNAS* **2018**, *115*, 12401-12406, doi:https://doi.org/10.1073/pnas.1812955115.

2. Wang, S.X.; Zhao, B.; Cai, S.Y.; Klimont, Z.; Nielsen, C.P.; Morikawa, T.; Woo, J.H.; Kim, Y.; Fu, X.; Xu, J.Y.; et al. Emission trends and mitigation options for air pollutants in East Asia. *Atmospheric chemistry and physics* **2014**, *14*, 6571-6603, doi:https://doi.org/10.5194/acp-14-6571-2014.

3. Liu, J.; Wang, L.; Zhu, Y.; Lin, C.-J.; Jang, C.; Wang, S.; Xing, J.; Yu, B.; Xu, H.; Pan, Y. Source attribution for mercury deposition with an updated atmospheric mercury emission inventory in the Pearl River Delta Region, China. *Frontiers of environmental science & engineering* **2019**, *13*, 1-14, doi:https://doi.org/10.1007/s11783-019-1087-6.

4. Emery, C.; Liu, Z.; Russell, A.G.; Odman, M.T.; Yarwood, G.; Kumar, N. Recommendations on statistics and benchmarks to assess photochemical model performance. *Journal of the Air & Waste Management Association (1995)* **2017**, *67*, 582-598, doi:https://doi.org/10.1080/10962247.2016.1265027.

5. Luo, Q.; Ren, Y.; Sun, Z.; Li, Y.; Li, B.; Yang, S.; Zhang, W.; Hu, Y.; Cheng, H. Atmospheric mercury pollution caused by fluorescent lamp manufacturing and the associated human health risk in a large industrial and commercial city. *Environmental pollution (1987)* **2021**, *269*, 116146, doi:https://doi.org/10.1016/j.envpol.2020.116146.

6. Chen, L.; Liu, M.; Xu, Z.; Fan, R.; Tao, J.; Chen, D.; Zhang, D.; Xie, D.; Sun, J. Variation trends and influencing factors of total gaseous mercury in the Pearl River Delta—A highly industrialised region in South China influenced by seasonal monsoons. *Atmospheric environment (1994)* **2013**, *77*, 757-766, doi:https://doi.org/10.1016/j.atmosenv.2013.05.053.

7. Wang, Z.-w.; Chen, Z.-s.; Duan, N.; Zhang, X.-s. Gaseous elemental mercury concentration in atmosphere at urban and remote sites in China. *Journal of environmental sciences (China)* **2007**, *19*, 176-180, doi:https://doi.org/10.1016/S1001-0742(07)60028-X.

8. Xu, H.; Zhu, Y.; Wang, L.; Lin, C.-J.; Jang, C.; Zhou, Q.; Yu, B.; Wang, S.; Xing, J.; Yu, L. Source contribution analysis of mercury deposition using an enhanced CALPUFF-Hg in the central Pearl River Delta, China. *Environmental pollution (1987)* **2019**, *250*, 1032-1043, doi:https://doi.org/10.1016/j.envpol.2019.04.008.

9. Huang, M.; Deng, S.; Dong, H.; Dai, W.; Pang, J.; Wang, X. Impacts of Atmospheric Mercury Deposition on Human Multimedia Exposure: Projection from Observations in the Pearl River Delta Region, South China. *Environmental science & technology* **2016**, *50*, 10625-10634, doi:https://doi.org/10.1021/acs.est.6b00514.

10. NBS. Key Data Bulletin of China's 1% Population Sample Survey in 2015. Available online: http://www.stats.gov.cn/tjsj/zxfb/201604/t20160420_1346151.html (accessed on 15 January 2021).

11. Guangzhou, W.; Jun, W. Economic and social impact of China's aging population and public policy response. *China economist (Beijing, China)* **2021**, *16*, 78-107, doi:https://doi.org/10.19602/j.chinaeconomist.2021.01.05.

12. China's 2020 Fertility and Adoption of a Three-Child Policy. *Population and development review* **2021**, *47*, 877-879, doi:https://doi.org/10.1111/padr.12434.

13. Tatum, M. China's three-child policy. *The Lancet (British edition)* **2021**, *397*, 2238-2238, doi:https://doi.org/10.1016/S0140-6736(21)01295-2.

14. Balfour, J.L.; Kaplan, G.A. Neighborhood Environment and Loss of Physical Function in Older Adults: Evidence from the Alameda County Study. *American Journal of Epidemiology* **2002**, *155*, 507-515 %@ 0002-9262, doi:https://doi.org/10.1093/aje/155.6.507.

15. Maio, S.; Sarno, G.; Baldacci, S.; Annesi-Maesano, I.; Viegi, G. Air quality of nursing homes and its effect on the lung health of elderly residents. *EXPERT REVIEW OF RESPIRATORY MEDICINE* **2015**, *9*, 671-673, doi:https://doi.org/10.1586/17476348.2015.1105742.

16. Sandstrom, T.; Frew, A.J.; Svartengren, M.; Viegi, G. The need for a focus on air pollution research in the elderly. *EUROPEAN RESPIRATORY JOURNAL* **2003**, *21*, 92S-95S, doi:https://doi.org/10.1183/09031936.03.00403503.

17. Annesi-Maesano, I.; Agabiti, N.; Pistelli, R.; Couilliot, M.F.; Forastiere, F. Subpopulations at increased risk of adverse health outcomes from air pollution. *EUROPEAN RESPIRATORY JOURNAL* **2003**, *21*, 57S-63S, doi:https://doi.org/10.1183/09031936.03.00402103.

18. EPA. Integrated Science Assessment for Particulate Matter (Final Report). Available online: https://cfpub.epa.gov/ncea/risk/recordisplay.cfm?deid=216546 (accessed on 20 June 2022).

19. EPA. Exposure Factors Handbook: 2011 Edition. Available online: https://nepis.epa.gov/Exe/ZyPURL.cgi?Dockey=P100LMCH.txt (accessed on 20 June 2022).

20. Annesi-Maesano, I.; Hulin, M.; Lavaud, F.; Raherison, C.; Kopferschmitt, C.; de Blay, F.; André Charpin, D.; Denis, C. Poor air quality in classrooms related to asthma and rhinitis in primary schoolchildren of the French 6 Cities Study. *Thorax* **2012**, *67*, 682-688, doi:https://doi.org/10.1136/thoraxjnl-2011-200391.

21. Clark, N.A.; Demers, P.A.; Karr, C.J.; Koehoorn, M.; Lencar, C.; Tamburic, L.; Brauer, M. Effect of Early Life Exposure to Air Pollution on Development of Childhood Asthma. *Environmental health perspectives* **2010**, *118*, 284-290, doi:https://doi.org/10.1289/ehp.0900916.

22. Song, W.; Li, Y.; Hao, Z.; Li, H.; Wang, W. Public health in China: An environmental and socio-economic perspective. *Atmospheric Environment* **2016**, *129*, 9-17, doi:https://doi.org/10.1016/j.atmosenv.2015.12.021.

23. Whyte, M.K. Soaring Income Gaps: China in Comparative Perspective. *Daedalus (Cambridge, Mass.)* **2014**, *143*, 39-52, doi:https://doi.org/10.1162/DAED_a_00271.

24. Szaflarski, M. The Impact of Inequality: How to Make Sick Societies Healthier. *Preventing Chronic Disease* **2005**, *3*, 477-479.

25. Wright, T. The Political Economy of Coal Mine Disasters in China: "Your Rice Bowl or Your Life". *The China quarterly (London)* **2004**, *179*, 629-646, doi:https://doi.org/10.1017/S0305741004000517.